Published by Avanti Publishers

Journal of Advances in Applied & Computational Mathematics

ISSN (online): 2409-5761

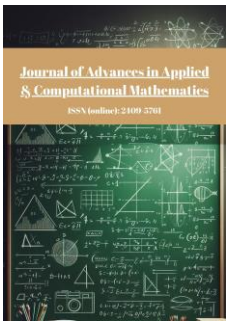

Novel Exact Traveling Wave Solutions of the (2+1)-Dimensional Calogero-Bogoyavlenskii-Schiff Equation via the Kumar-Malik and Improved F-Expansion Methods

Yiting Hu[1,*], Yuqiang Feng[1] and Jun Jiang[2]

[1]*School of Science, Wuhan University of Science and Technology, Wuhan 430081, Hubei, China*

[2]*Hubei Province Key Laboratory of Systems Science in Metallurgical Process, Wuhan 430081, Hubei, China*

ARTICLE INFO

Article Type: Research Article

Academic Editor: Shabir Ahmad

Keywords:
Kumar-Malik method
Traveling wave solutions
Nonlinear evolution equations
Improved F-expansion method
Calogero-Bogoyavlenskii-Schiff equation

Timeline:
Received: January 20, 2026
Accepted: February 27, 2026
Published: April 01, 2026

Citation: Hu Y, Feng Y, Jiang J. Novel exact traveling wave solutions of the (2+1)-dimensional Calogero-Bogoyavlenskii-Schiff equation via the Kumar-Malik and improved F-expansion methods. J Adv Appl Computat Math. 2026; 13(1): 32-53.

DOI: https://doi.org/10.15377/2409-5761.2026.13.3

ABSTRACT

This paper presents a rigorous investigation of analytical solutions for the (2+1)-dimensional Calogero-Bogoyavlenskii-Schiff (CBS) equation. To systematically analyze the nonlinear wave structures inherent in the CBS equation, we innovatively employ both the Kumar-Malik method and an improved F-expansion method, successfully constructing multiple families of exact solutions, including hyperbolic functions, trigonometric functions, and rational functions. Using the powerful mapping capabilities of Maple software, the obtained solutions are visualized as 3D plots, 2D graphs, and contour maps; through detailed analysis, kink wave solutions, singular periodic wave solutions, and rational singular solutions are clearly identified. These findings not only significantly expand the solution space for the integer-order CBS equation but also provide fresh theoretical insights into its dynamical characteristics. The results are expected to stimulate new research directions and facilitate substantial progress in nonlinear wave theory.

*Corresponding Author
Email: 164772549@qq.com
Tel: +(86) 13477457493

1. Introduction

While linear equations are limited to describing simple, superposition-compliant phenomena, nonlinear partial differential equations (NPDEs) provide a powerful mathematical framework for characterizing real-world nonlinear effects. Through analytical or numerical methods, NPDEs reveal the intrinsic evolutionary laws of complex systems, serving as a fundamental tool for modeling intricate physical phenomena and dynamical systems [1-3]. For instance, the Korteweg-de Vries (KdV) equation [4] was the first to mathematically explain the counterintuitive phenomenon of soliton propagation, where isolated waves maintain stable waveforms over long distances due to a precise balance between nonlinearity and dispersion. Meanwhile, the Navier–Stokes equations [5] incorporate nonlinear convection as a key mechanism governing turbulent fluid dynamics, underpinning critical applications such as aerodynamic design, typhoon trajectory prediction, and ocean circulation modeling. As a simplified model, the Burgers equation [6] facilitates the analysis of shock wave formation and has been widely applied in studies of traffic flow dynamics and congestion evolution.

In the field of mathematical physics, the solution of nonlinear partial differential equations has been one of the core focuses of research, attracting many scholars to devote themselves to it, and fruitful results have been achieved in recent years. A series of well-established methods such as the variational iteration method [7-11], the (G'/G)-expansion method [12-15], the improved F-expansion method [16-20], the trial equation method [21-24], the homogeneous balance method [25-28], the Hirota bilinear method [29-32], and the improved Kudryashov's method [33-36] have been proposed one after another and continuously improved. These methods provide powerful tools to unlock the complex mathematical structure of NPDEs and reveal the physical laws underlying them.

The CBS equation studied in this paper is as follows:

$$u_{xt} + u_{xxxy} + au_x u_{xy} + bu_{xx} u_y = 0. \tag{1}$$

The Calogero-Bogoyavlenskii-Schiff equation [37] is an important nonlinear evolutionary model that describes the propagation of Riemannian waves, with established applications in fluid dynamics and plasma physics. This equation characterizes the interaction between a long wave propagating along the x-axis and Riemannian waves along the y-axis. In fluid dynamics, it provides a mathematical framework for cross-scale energy transfer between shallow water waves and internal waves; in plasma physics, it captures the nonlinear resonance between magnetoacoustic and ion-acoustic waves; in nonlinear optics, it describes waveform distortions of ultrashort pulses arising from the self-steepening effect in photonic crystal fibers. Owing to its ability to model these diverse wave phenomena, the CBS equation has attracted sustained research interest [38] and remains an active subject of study in mathematical physics.

While earlier studies on the CBS equation have successfully advanced our understanding of its nonlinear dynamics-such as investigating exact solutions across different dimensions [39], applying the symmetry method to reduce the governing equation into solvable ordinary differential equations [40], and employing the bilinear method to derive multiple-soliton structures [41] these approaches typically target specific solution classes. The present study advances beyond these works in two key aspects: First, instead of employing disjoint analytical methods for different wave types, we establish a conceptually unified framework that simultaneously derives kink, singular periodic, and rational waves. Second, our solutions incorporate a broader spectrum of arbitrary coefficients, which offers enhanced parameter flexibility. This property facilitates a clearer observation of wave structure variations and provides a useful analytical tool to characterize nonlinear wave propagation across diverse physical conditions. For a direct and systematic overview of these distinguishing features, readers are referred to the comparison table in **Appendix B**.

Recently, Sachin Kumar [42] innovatively proposed a new analytical method, which opens a new path for the creation of exact solutions of high-dimensional nonlinear partial differential equations. Inspired by this, this study aims to apply the Kumar-Malik method to explore the integer order CBS equation in depth in an attempt to construct more different types of analytical solutions to further enrich the knowledge of the dynamical behavior of this equation. Moreover, the improved F-expansion method [43-46] is also an effective tool for solving the exact solution

of nonlinear evolution equations. Based on the traditional F-expansion method, the improved F-expansion method transforms the original nonlinear partial differential equation into an ordinary differential equation by introducing an appropriate traveling wave transform. Subsequently, combining with higher-order auxiliary equations, further richer and more diverse forms of exact solutions are obtained.

The principal innovations of this research can be summarized as follows:

1. Through the innovative combination of the Kumar-Malik method and an enhanced F-expansion technique, we establish an efficient and systematic solution framework. This approach markedly improves both the construction efficiency and the structural diversity of analytical solutions for the CBS equation, offering a unified perspective for solving high-dimensional nonlinear evolution equations.

2. For the first time, we have systematically derived a comprehensive family of composite exact solutions for the integer-order CBS equation under this framework. Notably, we obtained physically robust kink wave solutions, singular periodic wave solutions, and rational singular solutions with broad parameter spaces, thereby substantially enriching the known dynamical properties of this equation.

3. The derived exact solutions possess not only mathematical significance but also provide a new theoretical framework for analyzing nonlinear wave propagation phenomena in various physical systems, particularly in fluid dynamics and plasma physics.

This paper is divided into the following sections: In Section 2, the specific procedure of the Kumar-Malik method is outlined. In Section 3, a large number of exact solutions of the CBS equation are obtained by the Kumar-Malik method. In Section 4, analytical solutions of the CBS equation are obtained by the improved F-expansion method. In Section 5, we give 3D plots, 2D graphs, and contour maps of some of the solutions using Maple. In Section 6, stability analysis is discussed. Finally, in Section 7, the conclusions of this paper are presented.

2. Content Steps of the Kumar-Malik Method

In this section, we introduce the Kumar-Malik method. First, let us consider that we have an NLPDE of the form:

$$G(u,u_{x,}u_t,u_{xx},u_{xt},u_{tt},\cdots)=0, \tag{2}$$

where $u=u(x,t)$ is an unknown function containing x and t .

Step 1: We perform the following traveling wave transformation:

$$u(x,y,t)=v(\xi),\ \xi=x+\omega y-rt, \tag{3}$$

Here, ω,r represent constant coefficients. Substituting Eq. (3) into Eq. (2), we obtain the following ordinary differential equation:

$$F(v,v^{'},v^{''},v^{'''},\cdots)=0. \tag{4}$$

Step 2: Assume that Eq. (4) has a solution of the following form:

$$v(\xi)=L_0+L_1\Theta(\xi)+L_2\Theta(\xi)^2+\ldots+L_N\Theta(\xi)^N, \tag{5}$$

where the L_i (i=1,2,..,N) and $\Theta(\xi)$ satisfy the following first-order differential equation:

$$[\Theta^{'}(\xi)]^2=\beta_1\Theta^4(\xi)+\beta_2\Theta^3(\xi)+\beta_3\Theta^2(\xi)+\beta_4\Theta(\xi)+\beta_5, \tag{6}$$

where β_i (i= 1,2,..,5) are arbitrary constants.

Step 3: The value of N can be determined by applying the balancing principle in Eq. (4).

Step 4: Substituting Eq. (5) and its derivatives into Eq. (3) yields a polynomial in $\Theta(\xi)\Theta'(\xi)$. By collecting all coefficients of like powers and setting them equal to zero, we derive an algebraic system involving β_i (i=1,2,..,5). Solving this system leads to exact solutions of Eq. (4).

Step 5: Finally, we can use the transformed solutions of Eq. (3) and Eq. (4) to create an analytic solution of Eq. (2). Next, we give the exact solution of Eq. (6) by considering that there are four different cases as follows. For convenience, we will use the following notation throughout this article.

$$h_1 = 4\beta_1\beta_3 - {\beta_2}^2, \quad h_2 = 16\beta_1\beta_3 - 5{\beta_2}^2, \quad h_3 = 8\beta_1\beta_3 - 3{\beta_2}^2. \tag{7}$$

Case 1: $\beta_4 = \dfrac{\beta_2 h_1}{8{\beta_1}^2}, \beta_5 = 0$. Then Eq. (6) has the following Jacobi elliptic solutions:

Set 1.1. $\beta_1 < 0, h_1 > 0$

$$\Theta_{1,1,1}(\xi) = \frac{-\beta_2}{4\beta_1} \pm \frac{\beta_2}{4\beta_1} cn\left(\frac{\sqrt{-\beta_1 h_1}}{2\beta_1}\xi, \frac{\beta_2}{2\sqrt{h_1}}\right), \tag{8}$$

$$\Theta_{1,1,2}(\xi) = -\frac{\beta_2}{4\beta_1} \pm \frac{\beta_2}{4\beta_1} dn\left(\frac{\beta_2}{4\sqrt{-\beta_1}}\xi, \frac{2\sqrt{h_1}}{\beta_2}\right). \tag{9}$$

Set 1.2. $\beta_1 < 0, h_1 < 0, h_2 < 0$

$$\Theta_{1,2,1}(\xi) = \frac{-\beta_2}{4\beta_1} \pm \frac{\sqrt{-h_2}}{4\beta_1} cn\left(\frac{\sqrt{\beta_1 h_1}}{2\beta_1}\xi, \frac{\sqrt{h_2 h_2}}{2h_1}\right), \tag{10}$$

$$\Theta_{1,2,2}(\xi) = \frac{-\beta_2}{4\beta_1} \pm \frac{\sqrt{-h_2}}{4\beta_1} dn\left(\frac{\sqrt{\beta_1 h_2}}{4\beta_2}\xi, \frac{2\sqrt{h_1 h_2}}{h_2}\right). \tag{11}$$

Set 1.3. $\beta_1 < 0, h_1 > 0, h_2 < 0$

$$\Theta_{1,3,1}(\xi) = \frac{-\beta_2}{4\beta_1} \pm \frac{\sqrt{-h_2}}{4\beta_1} nc\left(\frac{\sqrt{-\beta_1 h_1}}{2\beta_1}\xi, \frac{\beta_2}{2\sqrt{h_1}}\right), \tag{12}$$

$$\Theta_{1,3,2}(\xi) = \frac{-\beta_2}{4\beta_1} \pm \frac{\sqrt{-h_2}}{4\beta_1} nd\left(\frac{\beta_2}{4\sqrt{-\beta_1}}\xi, \frac{2\sqrt{h_1}}{\beta_2}\right). \tag{13}$$

Set 1.4. $\beta_1 h_1 > 0, h_1 h_2 > 0$

$$\Theta_{1,4,1}(\xi) = \frac{-\beta_2}{4\beta_1} \pm \frac{\beta_2}{4\beta_1} nc\left(\frac{\sqrt{\beta_1 h_1}}{2\beta_1}\xi, \frac{\sqrt{h_1 h_2}}{2h_1}\right), \tag{14}$$

$$\Theta_{1,4,2}(\xi)=\frac{-\beta_2}{4\beta_1}\pm\frac{\beta_2}{4\beta_1}nd(\frac{\sqrt{\beta_1 h_2}}{4\beta_1}\xi,\frac{2\sqrt{h_1 h_2}}{h_2}). \tag{15}$$

Set 1.5. $\beta_1>0,h_2<0$

$$\Theta_{1.5.1}(\xi)=\frac{-\beta_2}{4\beta_1}\pm\frac{\beta_2}{4\beta_1}ns(\frac{\beta_2}{4\sqrt{\beta_1}}\xi,\frac{\sqrt{-h_2}}{\beta_2}), \tag{16}$$

$$\Theta_{1.5.2}(\xi)=\frac{-\beta_2}{4\beta_1}\pm\frac{\sqrt{-h_2}}{4\beta_1}ns(\frac{\sqrt{-\beta_1 h_2}}{4\beta_1}\xi,\frac{\beta_2}{\sqrt{-h_2}}), \tag{17}$$

$$\Theta_{1.5.3}(\xi)=\frac{-\beta_2}{4\beta_1}\pm\frac{\sqrt{-h_2}}{4\beta_1}sn(\frac{\beta_2}{4\sqrt{\beta_1}}\xi,\frac{\sqrt{-h_2}}{\beta_2}), \tag{18}$$

$$\Theta_{1,5,4}(\xi)=\frac{-\beta_2}{4\beta_1}\pm\frac{\beta_2}{4\beta_1}sn(\frac{\sqrt{-\beta_1 h_2}}{4\beta_1}\xi,\frac{\beta_2}{\sqrt{-h_2}}). \tag{19}$$

Case 2: $\beta_4=\frac{\beta_2 h_1}{8{\beta_1}^2},\beta_5=\frac{{h_1}^2}{64{\beta_1}^3}$, Eq. (6) has the following triangular and hyperbolic solutions:

Set 2.1. $\beta_1>0,h_3<0$

$$\Theta_{2.1.1}(\xi)=\frac{-\beta_2}{4\beta_1}\pm\frac{\sqrt{-h_3}}{4\beta_1}\tanh(\frac{\sqrt{-\beta_1 h_3}}{4\beta_1}\xi), \tag{20}$$

$$\Theta_{2.1.2}(\xi)=\frac{-\beta_2}{4\beta_1}\pm\frac{\sqrt{-h_3}}{4\beta_1}\coth(\frac{\sqrt{-\beta_1 h_3}}{4\beta_1}\xi). \tag{21}$$

Set 2.2. $\beta_1>0,h_3>0$

$$\Theta_{2.2.1}(\xi)=\frac{-\beta_2}{4\beta_1}\pm\frac{\sqrt{h_3}}{4\beta_1}\tan(\frac{\sqrt{\beta_1 h_3}}{4\beta_1}\xi), \tag{22}$$

$$\Theta_{2.2.2}(\xi)=\frac{-\beta_2}{4\beta_1}\pm\frac{\sqrt{h_3}}{4\beta_1}\cot(\frac{\sqrt{\beta_1 h_3}}{4\beta_1}\xi). \tag{23}$$

Case 3: $\beta_4=\frac{\beta_2 h_1}{8{\beta_1}^2},\beta_5=\frac{{\beta_2}^2 h_2}{256{\beta_1}^3}$, Eq. (6) has the following triangular and hyperbolic solutions:

Set 3.1. $\beta_1<0,h_3<0$

$$\Theta_{3.1.1}(\xi)=\frac{-\beta_2}{4\beta_1}\pm\frac{\sqrt{-2h_3}}{4\beta_1}sech(\frac{\sqrt{2\beta_1 h_3}}{4\beta_1}\xi). \tag{24}$$

Set 3.2. $\beta_1 < 0, h_3 > 0$

$$\Theta_{3.2.1}(\xi) = \frac{-\beta_2}{4\beta_1} \pm \frac{\sqrt{-2h_3}}{4\beta_1} csch(\frac{\sqrt{2\beta_1 h_3}}{4\beta_1}\xi). \tag{25}$$

Set 3.3. $\beta_1 < 0, h_3 < 0$

$$\Theta_{3.3.1}(\xi) = \frac{-\beta_2}{4\beta_1} \pm \frac{\sqrt{-2h_3}}{4\beta_1} \sec(\frac{\sqrt{-2\beta_1 h_3}}{4\beta_1}\xi), \tag{26}$$

$$\Theta_{3.3.2}(\xi) = \frac{-\beta_2}{4\beta_1} \pm \frac{\sqrt{-2h_3}}{4\beta_1} \csc(\frac{\sqrt{-2\beta_1 h_3}}{4\beta_1}\xi). \tag{27}$$

3. Application of Kumar-Malik Method to the CBS Equation

In this section, we use the Kumar-Malik method to solve the CBS equation. Let us consider the following traveling wave transform:

$$u(x,y,t) = v(\xi), \xi = x + \omega y - rt, \tag{28}$$

Here ω and r are constants and substituting the above transformations into Eq. (1) yields

$$\omega v''' - rv'' + (a+b)\omega v' v'' = 0. \tag{29}$$

Integrating both sides of Eq. (29) yields

$$\omega v'' - rv' + \frac{1}{2}(a+b)\omega (v')^2 = M. \tag{30}$$

By setting M=0 and substituting $\phi(\xi)$ with v', Eq. (30) is converted to the following second-order ordinary differential equation:

$$\omega \phi'' - r\phi + \frac{1}{2}(a+b)\omega \phi^2 = 0. \tag{31}$$

According to the homogeneous balance principle [47-50], from Eq. (31), we have $N = 2$ and

$$\phi(\xi) = L_0 + L_1\Theta(\xi) + L_2\Theta(\xi)^2, \tag{32}$$

Substituting Eq. (32) and Eq. (6) into Eq. (31), we get the following system of equations:

$$\begin{cases} \Theta^4(\xi): & 6\omega L_2\beta_1 + \frac{1}{2}(a+b)\omega L_2^2 = 0, \\ \Theta^3(\xi): & \omega(2L_1\beta_1 + 5L_2\beta_2) + (a+b)\omega L_1 L_2 = 0, \\ \Theta^2(\xi): & \omega\left(\frac{3}{2}\beta_2 L_1 + 4L_2\beta_2\right) - rL_2 + \frac{1}{2}(a+b)\omega(L_1^2 + 2L_0 L_2) = 0, \\ \Theta^1(\xi): & \omega(\beta_3 L_1 + 3L_2\beta_4) - rL_1 + (a+b)\omega L_0 L_1 = 0, \\ \Theta^0(\xi): & \omega\left(\frac{1}{2}L_1 + 2L_2\beta_5\right) - rL_0 + \frac{1}{2}(a+b)\omega L_0^2 = 0. \end{cases} \tag{33}$$

By solving the above system of equations we get

$$L_0 = \frac{-(\beta_2\beta_3 + 6\beta_1\beta_4) + \sqrt{\beta_2^2\beta_3^2 + 12\beta_1\beta_2\beta_3\beta_4 + 36\beta_1^2\beta_4^2 - 6\beta_2^3\beta_4 - 48\beta_1\beta_2^2\beta_5}}{(a+b)\beta_2},$$

$$L_1 = \frac{-6\beta_2}{a+b},$$

$$L_2 = \frac{-12\beta_1}{a+b},$$

$$r = \omega\left(\frac{6\beta_1\beta_4}{\beta_2} + \beta_3 + (a+b)L_0\right). \tag{34}$$

Case 1: $\beta_4 = \frac{\beta_2 h_1}{8\beta_1^2}, \beta_5 = 0$. Then Eq. (1) has the following Jacobi elliptic solutions:

Set 1.1. $\beta_1 < 0, h_1 > 0$

$$\phi_{1.1.1}(x,y,t) = \frac{\left(\begin{array}{l} 3\beta_2{}^3(1 - \mathrm{cn}^2\left(\frac{\sqrt{-\beta_1(4\beta_1\beta_3 - \beta_2{}^2)}}{2\beta_1}(x + \omega y - rt), \frac{\beta_2}{2\sqrt{4\beta_1\beta_3 - \beta_2{}^2}}\right)) \\ + \sqrt{16\beta_2{}^2\beta_3{}^2 + (4\beta_1\beta_3 - \beta_2{}^2)(24\beta_1\beta_2\beta_3 + 9\beta_2{}^2(4\beta_1\beta_3 - \beta_2{}^2) - 12\beta_2{}^4)} \\ - (4\beta_1\beta_2\beta_3 + 3\beta_2(4\beta_1\beta_3 - \beta_2{}^2)) \end{array}\right)}{4(a+b)\beta_1\beta_2}, \tag{35}$$

$$\phi_{1.1.2}(x,y,t) = \frac{\left(\begin{array}{l} 3\beta_2{}^3(1 - dn^2\left(\frac{\beta_2}{4\sqrt{-\beta_1}}(x + \omega y - rt), \frac{2\sqrt{4\beta_1\beta_3 - \beta_2{}^2}}{\beta_2}\right)) \\ + \sqrt{16\beta_2{}^2\beta_3{}^2 + 24\beta_1\beta_2\beta_3(4\beta_1\beta_3 - \beta_2{}^2) + 9\beta_2{}^2(4\beta_1\beta_3 - \beta_2{}^2)^2 - 12\beta_2{}^4(4\beta_1\beta_3 - \beta_2{}^2)} \\ - (4\beta_1\beta_2\beta_3 + 3\beta_2(4\beta_1\beta_3 - \beta_2{}^2)) \end{array}\right)}{4(a+b)\beta_1\beta_2}. \tag{36}$$

Set 1.2. $\beta_1 < 0, h_1 < 0, h_2 < 0$

$$\phi_{1.2.1}(x,y,t) =$$

$$\frac{\left(\begin{array}{l}(48\beta_1\beta_2\beta_3-15\beta_2{}^3)cn^2\left(\frac{\sqrt{\beta_1(4\beta_1\beta_3-\beta_2{}^2)}}{2\beta_1}(x+\omega y-rt),K_1\right)\\+\sqrt{16\beta_2{}^2\beta_3{}^2+(4\beta_1\beta_3-\beta_2{}^2)\left(24\beta_1\beta_2\beta_3+9\beta_2{}^2(4\beta_1\beta_3-\beta_2{}^2)-12\beta_2{}^4\right)}\\-(4\beta_1\beta_2\beta_3+3\beta_2(4\beta_1\beta_3-\beta_2{}^2))+3\beta_2{}^3\end{array}\right)}{4(a+b)\beta_1\beta_2}, \tag{37}$$

where $K_1=\frac{\sqrt{(4\beta_1\beta_3-\beta_2{}^2)(16\beta_1\beta_3-5\beta_2{}^2)}}{2(4\beta_1\beta_3-\beta_2{}^2)}$.

$$\phi_{1.2.2}(x,y,t)=$$

$$\frac{\left(\begin{array}{l}(48\beta_1\beta_2\beta_3-15\beta_2{}^3)dn^2\left(\frac{\sqrt{\beta_1(16\beta_1\beta_3-5\beta_2{}^2)}}{2\beta_1}(x+\omega y-rt),K_2\right)\\+\sqrt{16\beta_2{}^2\beta_3{}^2+(4\beta_1\beta_3-\beta_2{}^2)(24\beta_1\beta_2\beta_3+9\beta_2{}^2(4\beta_1\beta_3-\beta_2{}^2)-12\beta_2{}^4)}\\-(4\beta_1\beta_2\beta_3+3\beta_2(4\beta_1\beta_3-\beta_2{}^2))+3\beta_2{}^3\end{array}\right)}{4(a+b)\beta_1\beta_2}, \tag{38}$$

where $K_2=\frac{2\sqrt{(4\beta_1\beta_3-\beta_2{}^2)(16\beta_1\beta_3-5\beta_2{}^2)}}{16\beta_1\beta_3-5\beta_2{}^2}$.

Set 1.3. $\beta_1<0,h_1>0,h_2<0$

$$\phi_{1.3.1}(x,y,t)=$$

$$\frac{\left(\begin{array}{l}(48\beta_1\beta_2\beta_3-15\beta_2{}^3)nc^2\left(\frac{\sqrt{-\beta_1(4\beta_1\beta_3-\beta_2{}^2)}}{2\beta_1}(x+\omega y-rt),\frac{\beta_2}{2\sqrt{4\beta_1\beta_3-\beta_2{}^2}}\right)\\+\sqrt{16\beta_2{}^2\beta_3{}^2+(4\beta_1\beta_3-\beta_2{}^2)(24\beta_1\beta_2\beta_3+9\beta_2{}^2(4\beta_1\beta_3-\beta_2{}^2)-12\beta_2{}^4)}\\-(4\beta_1\beta_2\beta_3+3\beta_2(4\beta_1\beta_3-\beta_2{}^2))+3\beta_2{}^3\end{array}\right)}{4(a+b)\beta_1\beta_2}, \tag{39}$$

$$\phi_{1.3.2}(x,y,t)=$$

$$\frac{\left(\begin{array}{l}(48\beta_1\beta_2\beta_3-15{\beta_2}^3)nd^2\left(\frac{\beta_2}{4\sqrt{-\beta_1}}(x+\omega y-rt),\frac{2\sqrt{4\beta_1\beta_3-{\beta_2}^2}}{\beta_2}\right)\\+\sqrt{16{\beta_2}^2{\beta_3}^2+(4\beta_1\beta_3-{\beta_2}^2)(24\beta_1\beta_2\beta_3+9{\beta_2}^2(4\beta_1\beta_3-{\beta_2}^2)-12{\beta_2}^4)}\\-(4\beta_1\beta_2\beta_3+3\beta_2(4\beta_1\beta_3-{\beta_2}^2))+3{\beta_2}^3\end{array}\right)}{4(a+b)\beta_1\beta_2}. \tag{40}$$

Set 1.4. $\beta_1 h_1>0, h_1 h_2>0$

$$\phi_{1.4.1}(x,y,t)=$$

$$\frac{\left(\begin{array}{l}3{\beta_2}^3(1-nc^2\left(\frac{\sqrt{\beta_1(4\beta_1\beta_3-{\beta_2}^2)}}{2\beta_1}(x+\omega y-rt),\frac{\sqrt{(4\beta_1\beta_3-{\beta_2}^2)(16\beta_1\beta_3-5{\beta_2}^2)}}{2(4\beta_1\beta_3-{\beta_2}^2)}\right)\\+\sqrt{16{\beta_2}^2{\beta_3}^2+24\beta_1\beta_2\beta_3(4\beta_1\beta_3-{\beta_2}^2)+9{\beta_2}^2(4\beta_1\beta_3-{\beta_2}^2)^2-12{\beta_2}^4(4\beta_1\beta_3-{\beta_2}^2)}\\-(4\beta_1\beta_2\beta_3+3\beta_2(4\beta_1\beta_3-{\beta_2}^2))\end{array}\right)}{4(a+b)\beta_1\beta_2}, \tag{41}$$

$$\phi_{1.4.2}(x,y,t)=$$

$$\frac{\left(\begin{array}{l}-3{\beta_2}^3nd^2\left(\frac{\sqrt{\beta_1(16\beta_1\beta_3-5{\beta_2}^2)}}{4\beta_1}(x+\omega y-rt),\frac{2\sqrt{(4\beta_1\beta_3-{\beta_2}^2)(16\beta_1\beta_3-5{\beta_2}^2)}}{16\beta_1\beta_3-5{\beta_2}^2}\right)\\+\sqrt{16{\beta_2}^2{\beta_3}^2+(4\beta_1\beta_3-{\beta_2}^2)(24\beta_1\beta_2\beta_3+9{\beta_2}^2(4\beta_1\beta_3-{\beta_2}^2)-12{\beta_2}^4)}\\-(4\beta_1\beta_2\beta_3+3\beta_2(4\beta_1\beta_3-{\beta_2}^2))+3{\beta_2}^3\end{array}\right)}{4(a+b)\beta_1\beta_2}. \tag{42}$$

Set 1.5. $\beta_1>0, h_2<0$

$$\phi_{1.5.1}(x,y,t)=$$

$$\frac{\left(\begin{array}{l}3{\beta_2}^3(1-ns^2\left(\frac{\beta_2}{4\sqrt{\beta_1}}(x+\omega y-rt),\frac{\sqrt{-(16\beta_1\beta_3-5{\beta_2}^2)}}{\beta_2}\right)\\+\sqrt{16{\beta_2}^2{\beta_3}^2+24\beta_1\beta_2\beta_3(4\beta_1\beta_3-{\beta_2}^2)+9{\beta_2}^2(4\beta_1\beta_3-{\beta_2}^2)^2-12{\beta_2}^4(4\beta_1\beta_3-{\beta_2}^2)}\\-(4\beta_1\beta_2\beta_3+3\beta_2(4\beta_1\beta_3-{\beta_2}^2))\end{array}\right)}{4(a+b)\beta_1\beta_2}, \tag{43}$$

$$\phi_{1.5.2}(x,y,t)=$$

$$\frac{\left(\begin{array}{l}(48\beta_1\beta_2\beta_3-15\beta_2{}^3)ns^2\left(\frac{\sqrt{-\beta_1(16\beta_1\beta_3-5\beta_2{}^2)}}{4\beta_1}(x+\omega y-rt),\frac{\beta_2}{\sqrt{5\beta_2{}^2-16\beta_1\beta_3}}\right)\\+\sqrt{16\beta_2{}^2\beta_3{}^2+24\beta_1\beta_2\beta_3(4\beta_1\beta_3-\beta_2{}^2)+9\beta_2{}^2(4\beta_1\beta_3-\beta_2{}^2)^2-12\beta_2{}^4(4\beta_1\beta_3-\beta_2{}^2)}\\-(4\beta_1\beta_2\beta_3+3\beta_2(4\beta_1\beta_3-\beta_2{}^2))+3\beta_2{}^3\end{array}\right)}{4(a+b)\beta_1\beta_2},\tag{44}$$

$$\phi_{1.5.3}(x,y,t)=$$

$$\frac{\left(\begin{array}{l}(48\beta_1\beta_2\beta_3-15\beta_2{}^3)sn^2\left(\frac{\beta_2}{4\sqrt{\beta_1}}(x+\omega y-rt),\frac{\sqrt{5\beta_2{}^2-16\beta_1\beta_3}}{\beta_2}\right)\\+\sqrt{16\beta_2{}^2\beta_3{}^2+24\beta_1\beta_2\beta_3(4\beta_1\beta_3-\beta_2{}^2)+9\beta_2{}^2(4\beta_1\beta_3-\beta_2{}^2)^2-12\beta_2{}^4(4\beta_1\beta_3-\beta_2{}^2)}\\-(4\beta_1\beta_2\beta_3+3\beta_2(4\beta_1\beta_3-\beta_2{}^2))+3\beta_2{}^3\end{array}\right)}{4(a+b)\beta_1\beta_2},\tag{45}$$

$$\phi_{1.5.4}(x,y,t)=$$

$$\frac{\left(\begin{array}{l}-3\beta_2{}^3sn^2\left(\frac{\sqrt{-\beta_1(16\beta_1\beta_3-5\beta_2{}^2)}}{4\beta_1}(x+\omega y-rt),\frac{\beta_2}{\sqrt{-16\beta_1\beta_3+5\beta_2{}^2}}\right)\\+\sqrt{16\beta_2{}^2\beta_3{}^2+24\beta_1\beta_2\beta_3(4\beta_1\beta_3-\beta_2{}^2)+9\beta_2{}^2(4\beta_1\beta_3-\beta_2{}^2)^2-12\beta_2{}^4(4\beta_1\beta_3-\beta_2{}^2)}\\-(4\beta_1\beta_2\beta_3+3\beta_2(4\beta_1\beta_3-\beta_2{}^2))+3\beta_2{}^3\end{array}\right)}{4(a+b)\beta_1\beta_2}.\tag{46}$$

Case 2: $\beta_4=\frac{\beta_2 h_1}{8\beta_1{}^2},\beta_5=\frac{h_1{}^2}{64\beta_1{}^3}$, Eq. (1) has the following triangular and hyperbolic solutions:

Set 2.1. $\beta_1>0,h_3<0$

$$\phi_{2.1.1}(x,y,t)=$$

$$\frac{\left(\begin{array}{l}3(8\beta_1\beta_2\beta_3-3\beta_2{}^3)\tanh^2\left(\frac{\sqrt{-\beta_1(8\beta_1\beta_3-3\beta_2{}^2)}}{4\beta_1}(x+\omega y-rt)\right)\\+\sqrt{16\beta_2{}^2\beta_3{}^2+24\beta_1\beta_2\beta_3(4\beta_1\beta_3-\beta_2{}^2)-3\beta_2{}^2(4\beta_1\beta_3-\beta_2{}^2)^2-12\beta_2{}^4(4\beta_1\beta_3-\beta_2{}^2)}\\-(4\beta_1\beta_2\beta_3+3\beta_2(4\beta_1\beta_3-\beta_2{}^2))+3\beta_2{}^3\end{array}\right)}{4(a+b)\beta_1\beta_2}.\tag{47}$$

Integrating the above equation with respect to $\xi = x + \omega y - rt$, and using the identity $\int \tanh^2(k\xi)d\xi = \xi - \frac{1}{k}\tanh(k\xi)$, we obtain the exact solution $u(x,y,t)$:

$$u_{2.1.1}(x,y,t) = \lambda_1(x+\omega y - rt) + \frac{3}{(a+b)}\sqrt{\frac{-h_3}{\beta_1}}\tanh\left(\frac{\sqrt{-\beta_1 h_3}}{4\beta_1}(x+\omega y - rt)\right) + C. \tag{48}$$

$$\phi_{2.1.2}(x,y,t) =$$

$$\frac{\left(\begin{array}{l} 3(8\beta_1\beta_2\beta_3 - 3\beta_2{}^3)\coth^2\left(\frac{\sqrt{-\beta_1(8\beta_1\beta_3 - 3\beta_2{}^2)}}{4\beta_1}(x+\omega y - rt)\right) \\ +\sqrt{16\beta_2{}^2\beta_3{}^2 + 24\beta_1\beta_2\beta_3(4\beta_1\beta_3 - \beta_2{}^2) - 3\beta_2{}^2(4\beta_1\beta_3 - \beta_2{}^2)^2 - 12\beta_2{}^4(4\beta_1\beta_3 - \beta_2{}^2)} \\ -(4\beta_1\beta_2\beta_3 + 3\beta_2(4\beta_1\beta_3 - \beta_2{}^2)) + 3\beta_2{}^3 \end{array}\right)}{4(a+b)\beta_1\beta_2}. \tag{49}$$

Integrating the above equation with respect to $\xi = x + \omega y - rt$, and using the identity $\int \coth^2(k\xi)d\xi = \xi - \frac{1}{k}\coth(k\xi)$, we obtain the exact solution $u(x,y,t)$:

$$u_{2.1.2}(x,y,t) = \lambda_1(x+\omega y - rt) + \frac{3}{(a+b)}\sqrt{\frac{-h_3}{\beta_1}}\coth\left(\frac{\sqrt{-\beta_1 h_3}}{4\beta_1}(x+\omega y - rt)\right) + C. \tag{50}$$

Set 2.2. $\beta_1 > 0, h_3 > 0$

$$\phi_{2.2.1}(x,y,t) =$$

$$\frac{\left(\begin{array}{l} -3(8\beta_1\beta_2\beta_3 - 3\beta_2{}^3)\tan^2\left(\frac{\sqrt{\beta_1(8\beta_1\beta_3 - 3\beta_2{}^2)}}{4\beta_1}(x+\omega y - rt)\right) \\ +\sqrt{16\beta_2{}^2\beta_3{}^2 + 24\beta_1\beta_2\beta_3(4\beta_1\beta_3 - \beta_2{}^2) - 3\beta_2{}^2(4\beta_1\beta_3 - \beta_2{}^2)^2 - 12\beta_2{}^4(4\beta_1\beta_3 - \beta_2{}^2)} \\ -(4\beta_1\beta_2\beta_3 + 3\beta_2(4\beta_1\beta_3 - \beta_2{}^2)) + 3\beta_2{}^3 \end{array}\right)}{4(a+b)\beta_1\beta_2}, \tag{51}$$

Integrating the above equation with respect to $\xi = x + \omega y - rt$, and using the identity $\int \tan^2(k\xi)d\xi = \frac{1}{k}\tan(k\xi) - \xi$, we obtain the exact solution $u(x,y,t)$:

$$u_{2.2.1}(x,y,t) = \lambda_1(x+\omega y - rt) - \frac{3}{(a+b)}\sqrt{\frac{h_3}{\beta_1}}\tan\left(\frac{\sqrt{\beta_1 h_3}}{4\beta_1}(x+\omega y - rt)\right) + C, \tag{52}$$

$$\phi_{2.2.2}(x,y,t)=$$

$$\frac{\left(\begin{array}{l}-3(8\beta_1\beta_2\beta_3-3\beta_2{}^3)\cot^2\left(\frac{\sqrt{\beta_1(8\beta_1\beta_3-3\beta_2{}^2)}}{4\beta_1}(x+\omega y-rt)\right)\\+\sqrt{16\beta_2{}^2\beta_3{}^2+24\beta_1\beta_2\beta_3(4\beta_1\beta_3-\beta_2{}^2)-3\beta_2{}^2(4\beta_1\beta_3-\beta_2{}^2)^2-12\beta_2{}^4(4\beta_1\beta_3-\beta_2{}^2)}\\-(4\beta_1\beta_2\beta_3+3\beta_2(4\beta_1\beta_3-\beta_2{}^2))+3\beta_2{}^3\end{array}\right)}{4(a+b)\beta_1\beta_2}. \tag{53}$$

Integrating the above equation with respect to $\xi=x+\omega y-rt$, and using the identity $\int\cot^2(k\xi)d\xi=-\xi-\frac{1}{k}\cot(k\xi)$, we obtain the exact solution $u(x,y,t)$:

$$u_{2.2.2}(x,y,t)=\lambda_1(x+\omega y-rt)+\frac{3}{(a+b)}\sqrt{\frac{h_3}{\beta_1}}\cot\left(\frac{\sqrt{\beta_1 h_3}}{4\beta_1}(x+\omega y-rt)\right)+C. \tag{54}$$

In this subsection, the linear coefficient λ_1 is defined as

$$\lambda_1=\frac{\sqrt{16\beta_2{}^2\beta_3{}^2+24\beta_1\beta_2\beta_3h_1-3\beta_2{}^2h_1^2-12\beta_2{}^4h_1}-3\beta_2h_1+20\beta_1\beta_2\beta_3-6\beta_2{}^3}{4(a+b)\beta_1\beta_2}.$$

Case 3: $\beta_4=\frac{\beta_2h_1}{8\beta_1{}^2},\beta_5=\frac{\beta_2{}^2h_2}{256\beta_1{}^3}$, Eq. (1) has the following triangular and hyperbolic solutions:

Set 3.1. $\beta_1<0,h_3<0$

$$\phi_{3.1.1}(x,y,t)=$$

$$\frac{\left(\begin{array}{l}3(8\beta_1\beta_2\beta_3-3\beta_2{}^3)sech^2\left(\frac{\sqrt{2\beta_1(8\beta_1\beta_3-3\beta_2{}^2)}}{4\beta_1}(x+\omega y-rt)\right)\\+\sqrt{16\beta_2{}^2\beta_3{}^2+(4\beta_1\beta_3-\beta_2{}^2)(24\beta_1\beta_2\beta_3+9\beta_2{}^2(4\beta_1\beta_3-\beta_2{}^2)-12\beta_2{}^4)+K_3}\\-(4\beta_1\beta_2\beta_3+3\beta_2(4\beta_1\beta_3-\beta_2{}^2))+3\beta_2{}^3\end{array}\right)}{4(a+b)\beta_1\beta_2}, \tag{55}$$

where $K_3=-3\beta_2{}^4(16\beta_1\beta_3-5\beta_2{}^2)$.

Integrating the above equation with respect to $\xi=x+\omega y-rt$, and using the identity $\int sech^2(k\xi)d\xi=\frac{1}{k}\tanh(k\xi)$, we obtain the exact solution $u(x,y,t)$:

$$u_{3.1.1}(x,y,t)=\lambda_2(x+\omega y-rt)+\frac{3}{(a+b)}\sqrt{\frac{h_3}{2\beta_1}}\tanh\left(\frac{\sqrt{2\beta_1 h_3}}{4\beta_1}(x+\omega y-rt)\right)+C. \tag{56}$$

Set 3.2. $\beta_1<0, h_3>0$

$$\phi_{3.2.1}(x,y,t)=$$

$$\frac{\left(\begin{array}{l}-3(8\beta_1\beta_2\beta_3-3\beta_2{}^3)csch^2\left(\frac{\sqrt{2\beta_1(8\beta_1\beta_3-3\beta_2{}^2)}}{4\beta_1}(x+\omega y-rt)\right)\\+\sqrt{16\beta_2{}^2\beta_3{}^2+(4\beta_1\beta_3-\beta_2{}^2)(24\beta_1\beta_2\beta_3+9\beta_2{}^2(4\beta_1\beta_3-\beta_2{}^2)-12\beta_2{}^4)+K_3}\\-(4\beta_1\beta_2\beta_3+3\beta_2(4\beta_1\beta_3-\beta_2{}^2))+3\beta_2{}^3\end{array}\right)}{4(a+b)\beta_1\beta_2}, \tag{57}$$

where $K_3=-3\beta_2{}^4(16\beta_1\beta_3-5\beta_2{}^2)$.

Integrating the above equation with respect to $\xi=x+\omega y-rt$, and using the identity $\int csch^2(k\xi)d\xi=-\frac{1}{k}\coth(k\xi)$, we obtain the exact solution $u(x,y,t)$:

$$u_{3.2.1}(x,y,t)=\lambda_2(x+\omega y-rt)+\frac{3}{(a+b)}\sqrt{\frac{h_3}{2\beta_1}}\coth\left(\frac{\sqrt{2\beta_1 h_3}}{4\beta_1}(x+\omega y-rt)\right)+C. \tag{58}$$

Set 3.3. $\beta_1<0, h_3<0$

$$\phi_{3.3.1}(x,y,t)=$$

$$\frac{\left(\begin{array}{l}6(8\beta_1\beta_2\beta_3-3\beta_2{}^3)\sec^2\left(\frac{\sqrt{-2\beta_1(8\beta_1\beta_3-3\beta_2{}^2)}}{4\beta_1}(x+\omega y-rt)\right)\\+\sqrt{16\beta_2{}^2\beta_3{}^2+(4\beta_1\beta_3-\beta_2{}^2)(24\beta_1\beta_2\beta_3+9\beta_2{}^2(4\beta_1\beta_3-\beta_2{}^2)-12\beta_2{}^4)+K_3}\\-(4\beta_1\beta_2\beta_3+3\beta_2(4\beta_1\beta_3-\beta_2{}^2))+3\beta_2{}^3\end{array}\right)}{4(a+b)\beta_1\beta_2}, \tag{59}$$

where $K_3=-3\beta_2{}^4(16\beta_1\beta_3-5\beta_2{}^2)$.

Integrating the above equation with respect to $\xi=x+\omega y-rt$, and using the identity $\int \sec^2(k\xi)d\xi=\frac{1}{k}\tan(k\xi)$, we obtain the exact solution $u(x,y,t)$:

$$u_{3.3.1}(x,y,t)=\lambda_2(x+\omega y-rt)+\frac{6}{(a+b)}\sqrt{\frac{-h_3}{2\beta_1}}\tan\left(\frac{\sqrt{-2\beta_1 h_3}}{4\beta_1}(x+\omega y-rt)\right)+C. \tag{60}$$

$$\phi_{3.3.2}(x,y,t)=$$

$$\frac{\left(\begin{array}{l}6(8\beta_1\beta_2\beta_3-3\beta_2{}^3)\csc^2\left(\frac{\sqrt{-2\beta_1(8\beta_1\beta_3-3\beta_2{}^2)}}{4\beta_1}(x+\omega y-rt)\right)\\+\sqrt{16\beta_2{}^2\beta_3{}^2+(4\beta_1\beta_3-\beta_2{}^2)(24\beta_1\beta_2\beta_3+9\beta_2{}^2(4\beta_1\beta_3-\beta_2{}^2)-12\beta_2{}^4)+K_3}\\-(4\beta_1\beta_2\beta_3+3\beta_2(4\beta_1\beta_3-\beta_2{}^2))+3\beta_2{}^3\end{array}\right)}{4(a+b)\beta_1\beta_2}, \tag{61}$$

where $K_3=-3\beta_2{}^4(16\beta_1\beta_3-5\beta_2{}^2)$.

Integrating the above equation with respect to $\xi=x+\omega y-rt$, and using the identity $\int\csc^2(k\xi)d\xi=-\frac{1}{k}\cot(k\xi)$, we obtain the exact solution $u(x,y,t)$:

$$u_{3.3.2}(x,y,t)=\lambda_2(x+\omega y-rt)-\frac{6}{(a+b)}\sqrt{\frac{-h_3}{2\beta_1}}\cot\left(\frac{\sqrt{-2\beta_1 h_3}}{4\beta_1}(x+\omega y-rt)\right)+C. \tag{62}$$

In this subsection, the linear coefficient λ_2 is defined as follows:

$$\lambda_2=\frac{\sqrt{16\beta_2{}^2\beta_3{}^2+h_1(24\beta_1\beta_2\beta_3+9\beta_2{}^2h_1-12\beta_2{}^4)+K_3}-(4\beta_1\beta_2\beta_3+3\beta_2h_1)+3\beta_2{}^3}{4(a+b)\beta_1\beta_2}.$$

4. Improved F-expansion Method in the CBS Equation

According to the improved theory of F-expansion method, we have

$$u(\xi)=\sum_{i=0}^{N}(A_i(p+\Phi(\xi))^i+B_i(p+\Phi(\xi))^{-i}), \tag{63}$$

where $\Phi=\Phi(\xi)$ is the solution of the following ordinary differential equation

$$\frac{d\Phi(\xi)}{d\xi}=\Phi(\xi)^2+\tau, \tag{64}$$

where $A_i, B_i(i=0,\ldots,N)$ are indeterminate coefficients to be solved for in subsequent steps, and the following analytic solutions are given.

Case I. $\tau<0$, Eq. (64) has the following hyperbolic solution:

$$\Phi_1(\xi)=-\sqrt{-\tau}\tanh(\sqrt{-\tau}\xi), \tag{65}$$

$$\Phi_2(\xi) = -\sqrt{-\tau}\cosh(\sqrt{-\tau}\xi). \tag{66}$$

Case II. $\tau > 0,$ Eq. (64) has the following triangular solution:

$$\Phi_3(\xi) = -\sqrt{\tau}\tan(\sqrt{\tau}\xi), \tag{67}$$

$$\Phi_4(\xi) = -\sqrt{\tau}\cot(\sqrt{\tau}\xi). \tag{68}$$

Case III. $\tau = 0,$ Eq. (64) possesses the following rational solutions:

$$\Phi_5(\xi) = -\frac{1}{\xi}. \tag{69}$$

According to the homogeneous balance principle, from Eq. (31), we have $N = 2$ and

$$\phi(\xi) = A_0 + A_1(P+\Phi) + A_2(P+\Phi)^2 + B_0 + B_1(P+\Phi)^{-1} + B_2(P+\Phi)^{-2}, \tag{70}$$

Substituting Eq. (70) and Eq. (64) into Eq. (31), we obtain an algebraic system. Solving this system yields solutions for the following coefficients:

Family 1.

$$A_0 = -\frac{12p^2}{a+b} - B_0, A_1 = 0, A_2 = 0,$$

$$B_0 = B_0, B_1 = \frac{24p^3}{a+b}, B_2 = \frac{-12p^4}{a+b}. \tag{71}$$

We can obtain the solutions of Eq. (1) as:

Case I. $\tau < 0,$ Eq. (1) has the following hyperbolic solution:

$$\phi_{4.1.1.1}(x,y,t) = \frac{12\tau p^2\tanh^2(\sqrt{-\tau}(x+\omega y-rt))}{(a+b)(p-\sqrt{-\tau}\tanh^2(\sqrt{-\tau}(x+\omega y-rt)))}. \tag{72}$$

Integrating the above equation with respect to $\xi = x+\omega y-rt$, we obtain the exact solution:

$$u_{4.1.1.1}(x,y,t) = \frac{12p^2}{(a+b)(p-\sqrt{-\tau})}\left(\tau\xi + \sqrt{p}(-\tau)^{1/4}\tanh^{-1}\left(\frac{(-\tau)^{1/4}}{\sqrt{p}}\tanh(\sqrt{-\tau}\xi)\right)\right) + C. \tag{73}$$

$$\phi_{4.1.1.2}(x,y,t) = \frac{12\tau p^2\cosh^2(\sqrt{-\tau}(x+\omega y-rt))}{(a+b)(p-\sqrt{-\tau}\cosh^2(\sqrt{-\tau}(x+\omega y-rt)))}, \tag{74}$$

Similarly, by integrating Eq. (74) with respect to $\xi = x+\omega y-rt$, the exact hyperbolic representation is determined:

$$u_{4.1.1.2}(x,y,t) = \frac{12p^2}{a+b}\left(\sqrt{-\tau}\xi - \frac{\sqrt{p}}{\sqrt{p-\sqrt{-\tau}}}\tanh^{-1}\left(\frac{\sqrt{p}\tanh(\sqrt{-\tau}\xi)}{\sqrt{p-\sqrt{-\tau}}}\right)\right) + C. \tag{75}$$

Case II. $\tau > 0,$ Eq. (1) has the following triangular solution:

$$\phi_{4.1.2.1}(x,y,t) = -\frac{12\tau p^2 \tan^2(\sqrt{\tau}(x+\omega y - rt))}{(a+b)(p+\sqrt{\tau}\tan^2(\sqrt{\tau}(x+\omega y - rt)))}, \tag{76}$$

Following the same integration procedure on Eq. (76), the exact triangular solution is obtained as:

$$u_{4.1.2.1}(x,y,t) = \frac{12p^2}{(a+b)(p-\sqrt{\tau})}\left(\tau\xi - \sqrt{p}\tau^{1/4}\arctan\left(\frac{\tau^{1/4}}{\sqrt{p}}\tan(\sqrt{\tau}\xi)\right)\right) + C. \tag{77}$$

$$\phi_{4.1.2.2}(x,y,t) = -\frac{12\tau p^2 \cot^2(\sqrt{\tau}(x+\omega y - rt))}{(a+b)(p-\sqrt{\tau}\cot^2(\sqrt{\tau}(x+\omega y - rt)))}, \tag{78}$$

Analogously, integrating the auxiliary function Eq. (78) directly yields:

$$u_{4.1.2.2}(x,y,t) = \frac{12p^2}{(a+b)(p+\sqrt{\tau})}\left(\tau\xi + \sqrt{p}\tau^{1/4}\tanh^{-1}\left(\frac{\sqrt{p}}{\tau^{1/4}}\tan(\sqrt{\tau}\xi)\right)\right) + C. \tag{79}$$

Case III. $\tau = 0,$ Eq. (1) possesses the following rational solutions:

$$\phi_{4.1.3.1}(x,y,t) = -\frac{12p^2}{(a+b)(p(x+\omega y - rt)-1)^2}, \tag{80}$$

By carrying out a straightforward integration on Eq. (80) with respect to ξ, we find the corresponding rational solution:

$$u_{4.1.3.1}(x,y,t) = \frac{12p}{(a+b)(p(x+\omega y - rt)-1)} + C. \tag{81}$$

Family 2.

$$A_0 = -\frac{12p^2}{a+b} - B_0, A_1 = \frac{24p}{a+b}, A_2 = \frac{-12}{a+b},$$
$$B_0 = B_0, B_1 = 0, B_2 = 0. \tag{82}$$

We can also obtain the solutions of Eq. (1) as:

Case I. $\tau < 0,$ Eq. (1) has the following hyperbolic solution:

$$\phi_{4.2.1.1}(x,y,t) = \frac{12\tau}{(a+b)}\tanh^2(\sqrt{-\tau}(x+\omega y - rt)). \tag{83}$$

By integrating the above expression with respect to $\xi = x + \omega y - rt$, the exact soliton wave is expressed as:

$$u_{4.2.1.1}(x,y,t) = \frac{12\tau}{a+b}\left(\xi - \frac{1}{\sqrt{-\tau}}\tanh(\sqrt{-\tau}\xi)\right) + C. \tag{84}$$

$$\phi_{4.2.1.2}(x,y,t)=\frac{12\tau}{(a+b)}\cosh^2(\sqrt{-\tau}(x+\omega y-rt)), \tag{85}$$

Likewise, the corresponding integral form yields:

$$u_{4.2.1.2}(x,y,t)=\frac{12\tau}{a+b}\left(\frac{\xi}{2}+\frac{1}{4\sqrt{-\tau}}\sinh(2\sqrt{-\tau}\xi)\right)+C. \tag{86}$$

Case II. $\tau>0,$ Eq. (1) has the following triangular solution:

$$\phi_{4.2.2.1}(x,y,t)=-\frac{12\tau}{(a+b)}\tan^2(\sqrt{\tau}(x+\omega y-rt)), \tag{87}$$

Through direct integration with respect to ξ, we get:

$$u_{4.2.2.1}(x,y,t)=-\frac{12\tau}{a+b}\left(\frac{1}{\sqrt{\tau}}\tan(\sqrt{\tau}\xi)-\xi\right)+C. \tag{88}$$

$$\phi_{4.2.2.2}(x,y,t)=-\frac{12\tau}{(a+b)}\cot^2(\sqrt{\tau}(x+\omega y-rt)), \tag{89}$$

Subsequently, evaluating the integral of Eq. (89) produces:

$$u_{4.2.2.2}(x,y,t)=\frac{12\tau}{a+b}\left(\xi+\frac{1}{\sqrt{\tau}}\cot(\sqrt{\tau}\xi)\right)+C. \tag{90}$$

Case III. $\tau=0,$ Eq. (1) possesses the following rational solutions:

$$\phi_{4.2.3.1}(x,y,t)=-\frac{12}{(a+b)(x+\omega y-rt)^2}, \tag{91}$$

Integrating this rational expression term by term, we arrive at the final formulation:

$$u_{4.2.3.1}(x,y,t)=\frac{12}{(a+b)(x+\omega y-rt)}+C. \tag{92}$$

5. Graphic Display

In this section, we present graphical representations of selected obtained solutions. Using Maple software, we visualize these solutions through 3D plots, 2D graphs, and contour maps. Beyond generating visualizations, Maple's symbolic computation capabilities were extensively utilized (as outlined in the algorithmic flowchart in Section 5) to verify the algebraic systems and critically confirm that substituting our derived analytical expressions back into the original CBS equation strictly yields zero, thereby achieving dual graphical and mathematical validation.

By setting $a=4,b=2$ in Eq. (1), we obtain the classical CBS equation in its standard form. Our study has constructed various types of exact solutions, including hyperbolic, trigonometric, and rational functional forms. To illustrate the dynamical behaviors of these wave structures, we select three representative cases for graphical display: a kink wave solution ($u_{2.1.1}$), a singular periodic wave solution ($u_{2.2.2}$), and a rational singular solution ($u_{4.1.3.1}$). Their 3D plots, 2D wave profiles, and contour maps are presented in the following figures.

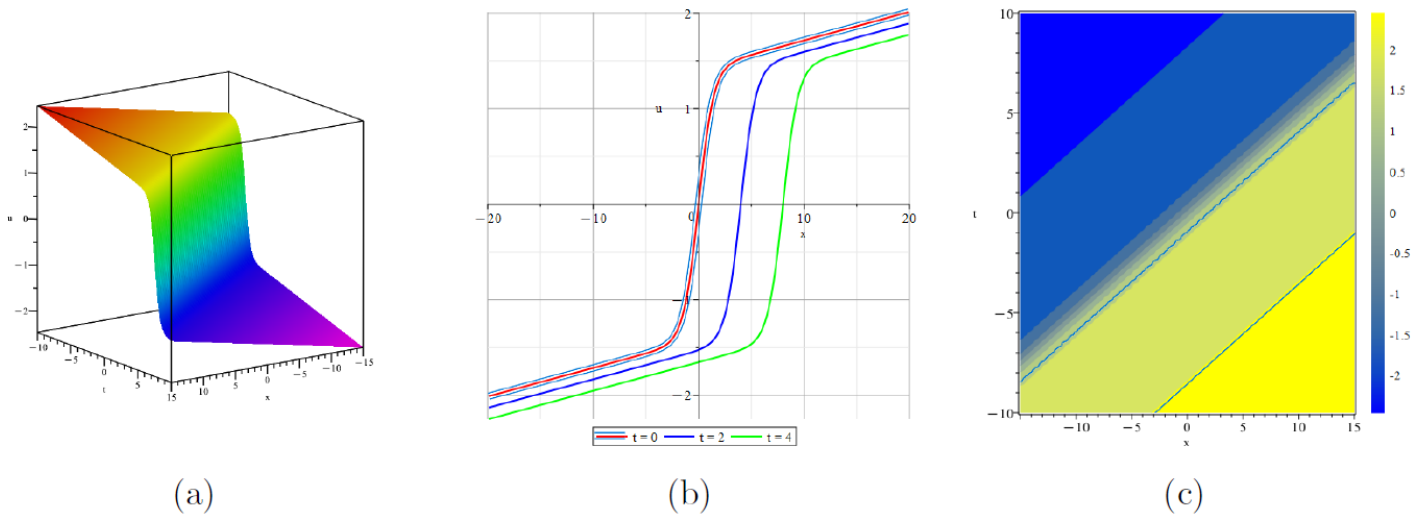

Figure 1: Visual interpretations of the solution $u_{2.1.1}(x,y,t)$ for Eq. (1) are presented: (**a**) 3D plot, (**b**) 2D plot, and (**c**) contour plot, where $\beta_1 = 1$, $\beta_2 = 2$, $\beta_3 = 0.5$, $a = 4$, $b = 2$, $\omega = 1$, $y = 0$, $C = 0$.

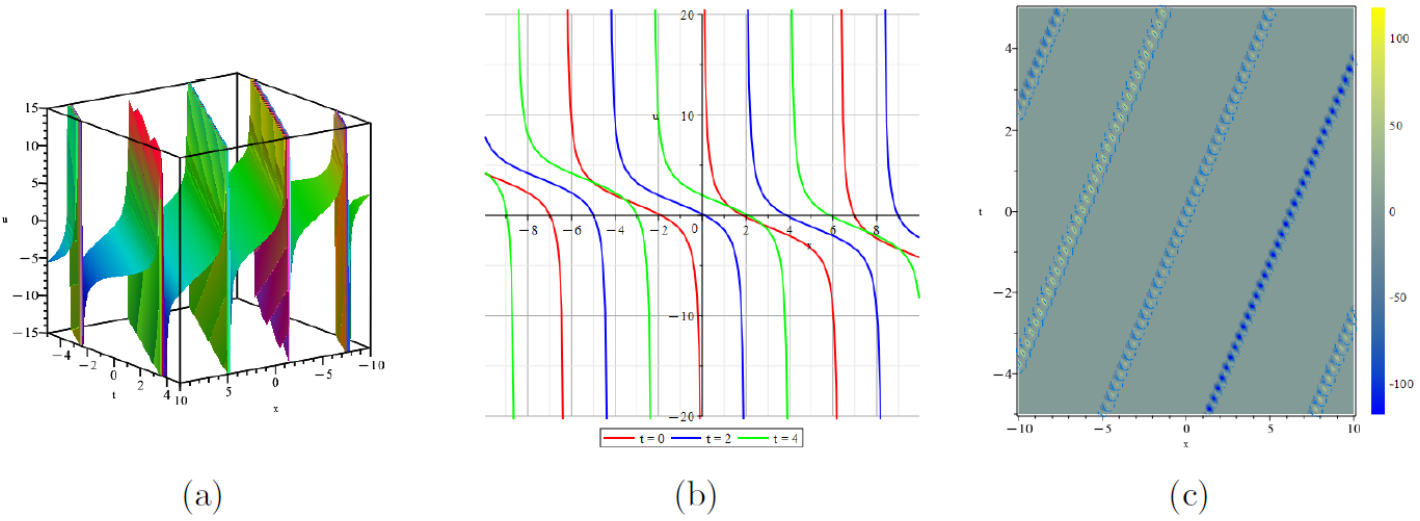

Figure 2: Visual interpretations of the solution $u_{2.2.2}(x,y,t)$ for Eq. (1) are presented: (**a**) 3D plot, (**b**) 2D plot, and (**c**) contour plot, where $\beta_1 = 1$, $\beta_2 = 2$, $\beta_3 = 2$, $a = 4$, $b = 2$, $\omega = 1$, $y = 0$, $C = 0$.

The 3D plot in Fig. (**1**) illustrates the evolutionary characteristics of the kink wave solution ($u_{2.1.1}$), which describes a smooth transition between two distinct asymptotic states superimposed on a linear background. This topological soliton maintains its wavefront profile during propagation, as confirmed by the shape-conservation property shown in the 2D plot. The contour map clearly reveals the linear trajectory of the kink, representing the steady-state propagation of a wavefront disturbance in nonlinear media. Fig. (**2**) displays the singular periodic wave ($u_{2.2.2}$), characterized by a series of repeating peaks that approach infinity. This pattern reflects the periodic instability and localized energy concentration inherent in certain nonlinear oscillating systems. The 3D undulations and the striped patterns in the contour plot quantitatively demonstrate the global periodicity and the recurring singular behavior of this trigonometric solution. Furthermore, the rational singular solution ($u_{4.1.3.1}$) is visualized in Fig. (**3**). Unlike smooth solitons, this solution exhibits a localized "blow-up" phenomenon where the amplitude becomes infinite at a singular point. The sharp isolated peak in the 3D plot and the corresponding high-intensity focus in the contour map capture the localization of an extreme event, which is of great significance in modeling wave collapse or energy focusing in fluids and plasmas. Together, these diverse wave structures-kink, singular periodic, and rational singular-reveal the rich and complex dynamical spectrum of the CBS equation.

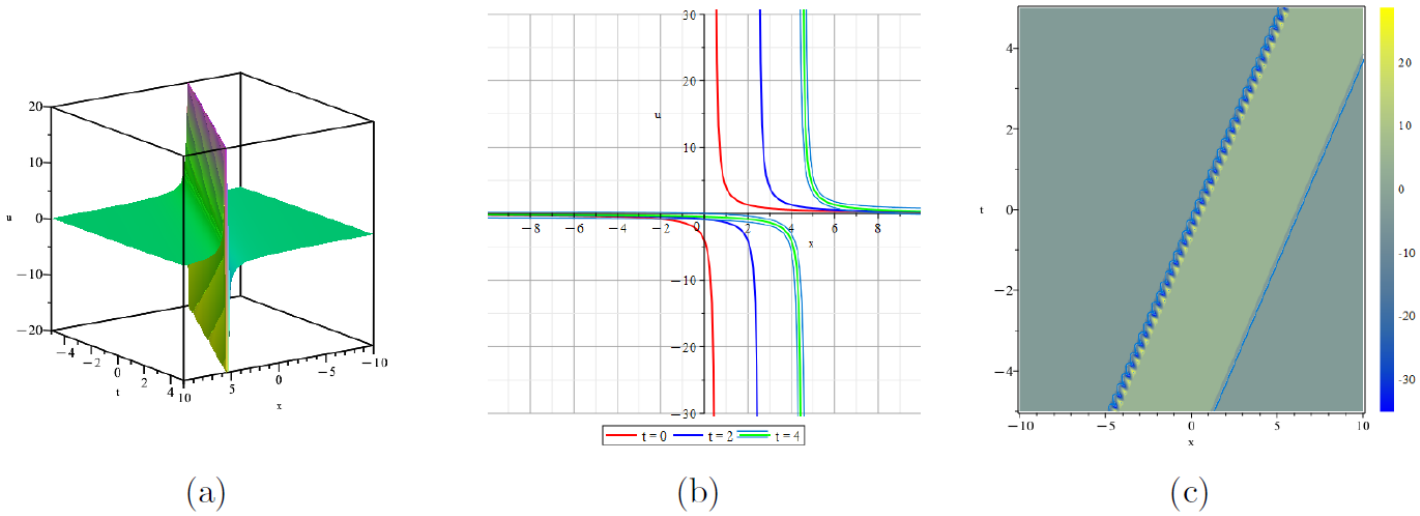

Figure 3: Visual interpretations of the solution $u_{4.1.3.1}(x,y,t)$ for Eq. (1) are presented: (**a**) 3D plot, (**b**) 2D plot, and (**c**) contour plot, where $p=2$, $a=4$, $b=2$, $\omega=1$, $y=0$, $C=0$.

6. Stability Analysis

Stability is a fundamental requirement for the mathematical and physical validity of exact solutions in nonlinear dispersive systems. In this section, we investigate the linear stability of Eq. (1). We employ the standard small perturbation expansion method from linear stability theory.

Let the perturbed solution be

$$u(x,y,t)=p+\varepsilon\delta(x,y,t), \tag{93}$$

where p is a constant background solution, $0<\varepsilon=1$ is a small perturbation parameter, and $\delta(x,y,t)$ denotes the weak disturbance.

Since p is constant, it is straightforward to verify that it satisfies Eq. (1). Substituting Eq. (93) into Eq. (1), we compute

$$\begin{gathered} u_x=\varepsilon\delta_x,\quad u_y=\varepsilon\delta_y,\quad u_t=\varepsilon\delta_t,\\ u_{xx}=\varepsilon\delta_{xx},\quad u_{xy}=\varepsilon\delta_{xy},\quad u_{xt}=\varepsilon\delta_{xt},\\ u_{xxxy}=\varepsilon\delta_{xxxy}. \end{gathered} \tag{94}$$

Substituting into Eq. (1) yields

$$\varepsilon\delta_{xt}+\varepsilon\delta_{xxxy}+a\varepsilon^2\delta_x\delta_{xy}+b\varepsilon^2\delta_{xx}\delta_y=0. \tag{95}$$

Neglecting higher-order terms $O(\varepsilon^2)$ and dividing by ε, we obtain the linearized equation

$$\delta_{xt}+\delta_{xxxy}=0. \tag{96}$$

To derive the dispersion relation, we assume a plane-wave solution of the form

$$\delta(x,y,t)=e^{i(hx+ly-vt)}, \tag{97}$$

where h and l are real wave numbers in the x- and y-directions, respectively, and v denotes the frequency.

Substituting Eq. (97) into Eq. (96), we obtain

$$(ih)(-iv)+(ih)^3(il)=0. \tag{98}$$

After simplification, this leads to the algebraic equation

$$hv+h^3l=0. \tag{99}$$

Solving for v, we obtain the dispersion relation

$$v=-h^2l. \tag{100}$$

From Eq. (100), it follows that v is real for all real wave numbers h and l. Therefore, the perturbation solution remains purely oscillatory in time and does not exhibit exponential growth or decay.

Consequently, the constant background solution $u=p$ is linearly stable. The above result shows that, at the linear level, the interplay between the mixed derivative term u_{xt} and the higher-order dispersive term u_{xxxy} does not induce modulation instability.

7. Conclusion

This study successfully applies the Kumar-Malik method and an improved F-expansion method to conduct in-depth investigation of the (2+1)-dimensional Calogero-Bogoyavlenskii-Schiff equation, systematically establishing effective approaches for simplifying and solving this complex nonlinear equation. Through these methods, we have successfully constructed a diverse array of exact solutions to the CBS equation, including hyperbolic solutions, trigonometric solutions, and rational function solutions. Among these, distinct wave structures such as kink waves, singular periodic waves, and rational singular solutions have been clearly identified and visualized. From the perspective of solution achievements, the newly obtained series of exact solutions significantly expands the solution space of the integer-order CBS equation. These novel solutions provide more comprehensive and precise mathematical descriptions enabling deeper insights into the physical phenomena governed by the CBS equation, such as the propagation and interaction of Riemann waves in hydrodynamics and plasma physics. The discovery of these diverse wave patterns contributes to clarifying the nonlinear dynamic behaviors of the system under varying conditions, thereby deepening our understanding of the intrinsic dynamical mechanisms of the CBS equation.

The research outcomes inject new vitality into scholarly investigations in related fields. They lay a solid theoretical foundation for subsequent scholars to explore potential applications of the CBS equation further, such as in simulations of more complex fluid and plasma systems. Simultaneously, these findings are expected to stimulate more innovative methodological research on solution approaches for nonlinear partial differential equations, promoting continuous advancement in this field and facilitating a more profound and comprehensive understanding of complex physical phenomena.

Conflict of Interest

The authors declare that there are no conflicts of interest, including any financial or personal relationships that could have influenced the work reported in this paper.

Funding

This research is partially supported by the Open Project of State Key Laboratory of Environment-friendly Energy Materials (19kfhg08).

Authors' Contributions

All authors contributed equally to the study.

References

[1] Iqbal M, Riaz MB, Rehman MA. Dynamical transitions and multistability in nonlinear wave systems: dual analytical insights into the geophysical Korteweg–de Vries equation. Model Earth Syst Environ. 2025; 11(6): 384. https://doi.org/10.1007/s40808-025-02559-w

[2] Li X, Sun Y, Guo P. Exploring the lossy nonlinear electrical transmission line model: soliton solutions via beta fractional derivative, unified F-expansion method, and dynamical insight. Int J Theor Phys. 2026; 65(2): 44. https://doi.org/10.1007/s10773-026-06267-8

[3] Jhangeer A, Abdelkader A. Noise-induced transitions in nonlinear oscillators: from quasi-periodic stability to stochastic chaos. Fractal Fract. 2025; 9(8): 550. https://doi.org/10.3390/fractalfract9080550

[4] Adjibi K, Martinez A, Mascorro M, Montes C, Oraby T, Sandoval R. Exact solutions of stochastic Burgers–Korteweg de Vries type equation with variable coefficients. Partial Differ Equ Appl Math. 2024; 11: 100753. https://doi.org/10.1016/j.padiff.2024.100753

[5] Brown DL, Cortez R, Minion ML. Accurate projection methods for the incompressible Navier–Stokes equations. J Comput Phys. 2001; 168(2): 464-99. https://doi.org/10.1006/jcph.2001.6715

[6] Oz F, Vuppala RK, Kara K, Gaitan F. Solving Burgers' equation with quantum computing. Quantum Inf Process. 2022; 21(1): 30. https://doi.org/10.1007/s11128-021-03391-8

[7] Noor MA, Mohyud-Din ST. Variational iteration method for fifth-order boundary value problems using He's polynomials. Math Probl Eng. 2008; 2008(1): 954794. https://doi.org/10.1155/2008/954794

[8] Momani S, Odibat Z. Numerical comparison of methods for solving linear differential equations of fractional order. Chaos Solitons Fractals. 2007; 31(5): 1248-55. https://doi.org/10.1016/j.chaos.2005.10.068

[9] Asaduzzaman M, Zger F, Kilicman A. Analytical approximate solutions to the nonlinear Fornberg–Whitham type equations via modified variational iteration method. Partial Differ Equ Appl Math. 2024; 9: 100631. https://doi.org/10.1016/j.padiff.2024.100631

[10] Yadav S, Singh M, Singh S, Heinrich S, Kumar J. Modified variational iteration method and its convergence analysis for solving nonlinear aggregation population balance equation. Comput Fluids. 2024; 274: 106233. https://doi.org/10.1016/j.compfluid.2024.106233

[11] Akrami MH, Poya A, Zirak MA. Solving the general form of the fractional Black–Scholes with two assets through reconstruction variational iteration method. Results Appl Math. 2024; 22: 100444. https://doi.org/10.1016/j.rinam.2024.100444

[12] Xu Y, Feng Y, Jiang J. Exact solutions of the fractional resonant nonlinear Schrödinger equation. Opt Quantum Electron. 2023; 55(13): 1208. https://doi.org/10.1007/s11082-023-05483-4

[13] Zayed EME, Gepreel KA. The (G'/G)-expansion method for finding traveling wave solutions of nonlinear partial differential equations in mathematical physics. J Math Phys. 2009; 50(1): 013502. https://doi.org/10.1063/1.3033750

[14] Zhang YL, Liu YP, Li ZB. A connection between the (G'/G)-expansion method and the truncated Painlevé expansion method and its application to the mKdV equation. Chin Phys B. 2010; 19(3): 030306. https://doi.org/10.1088/1674-1056/19/3/030306

[15] Zhang J, Jiang F, Zhao X. An improved (G'/G)-expansion method for solving nonlinear evolution equations. Int J Comput Math. 2010; 87(8): 1716-25. https://doi.org/10.1080/00207160802450166

[16] Zhou Y, Wang M, Wang Y. Periodic wave solutions to a coupled KdV equations with variable coefficients. Phys Lett A. 2003; 308(1): 31-6. https://doi.org/10.1016/S0375-9601(02)01775-9

[17] Ali Akbar M, Ali NHM. The improved F-expansion method with Riccati equation and its applications in mathematical physics. Cogent Math. 2017; 4(1): 1282577. https://doi.org/10.1080/23311835.2017.1282577

[18] He Y, Li S, Long Y. An improved F-expansion method and its application to Kudryashov–Sinelshchikov equation. Math Methods Appl Sci. 2014; 37(12): 1717-22. https://doi.org/10.1002/mma.2925

[19] Ozisik M, Secer A, Bayram M. On solitary wave solutions for the extended nonlinear Schrödinger equation via the modified F-expansion method. Opt Quantum Electron. 2023; 55(3): 215. https://doi.org/10.1007/s11082-022-04476-z

[20] Rabie WB, Ahmed HM. Constructing new soliton solutions for Kudryashov's quintuple self-phase modulation with dual-form of generalized nonlocal nonlinearity using extended F-expansion method. Opt Quantum Electron. 2023; 55(3): 233. https://doi.org/10.1007/s11082-022-04526-6

[21] Özyapici A. Generalized trial equation method and its applications to Duffing and Poisson–Boltzmann equations. Turk J Math. 2017; 41(3): 686-93. https://doi.org/10.3906/mat-1603-76

[22] Ekici M, Mirzazadeh M, Sonmezoglu A, Ullah MZ, Asma M, Zhou Q. Dispersive optical solitons with Schrödinger–Hirota equation by extended trial equation method. Optik. 2017; 136: 451-61. https://doi.org/10.1016/j.ijleo.2017.02.042

[23] Triki H, Wazwaz AM. Trial equation method for solving the generalized Fisher equation with variable coefficients. Phys Lett A. 2016; 380(13): 1260-2. https://doi.org/10.1016/j.physleta.2016.02.002

[24] Özyapici A, Bilgehan B. Generalized system of trial equation methods and their applications to biological systems. Appl Math Comput. 2018; 338: 722-32. https://doi.org/10.1016/j.amc.2018.06.020

[25] Wang M. Exact solutions for a compound KdV–Burgers equation. Phys Lett A. 1996; 213(5-6): 279-87. https://doi.org/10.1016/0375-9601(96)00103-X

[26] Tuffour F, Barnes B, Dontwi IK. The modified homogeneous balance methods for solving Korteweg–de Vries equations. Partial Differ Equ Appl Math. 2024; 13: 101035. https://doi.org/10.1016/j.padiff.2024.101035

[27] Eslami M, Fathi Vajargah B, Mirzazadeh M. Exact solutions of modified Zakharov–Kuznetsov equation by the homogeneous balance method. Ain Shams Eng J. 2014; 5(1): 221-5. https://doi.org/10.1016/j.asej.2013.06.005

[28] Rady ASA, Osman ES, Khalfallah M. The homogeneous balance method and its application to the Benjamin–Bona–Mahoney (BBM) equation. Appl Math Comput. 2010; 217(4): 1385-90. https://doi.org/10.1016/j.amc.2009.05.027

[29] Wazwaz AM. Burgers hierarchy: multiple kink solutions and multiple singular kink solutions. J Franklin Inst. 2010; 347(3): 618-26. https://doi.org/10.1016/j.jfranklin.2010.01.003

[30] Li W, Jiao A, Liu W, Guo Z. High-order rational-type solutions of the analogous (3+1)-dimensional Hirota-bilinear-like equation. Math Biosci Eng. 2023; 20(11): 19360-71. https://doi.org/10.3934/mbe.2023856

[31] Guo P, Wu X, Wang LB. Multiple soliton solutions for the variant Boussinesq equations. Adv Differ Equ. 2015; 2015: 37. https://doi.org/10.1186/s13662-015-0371-4

[32] Li CY. An improved Hirota bilinear method and new application for a nonlocal integrable complex modified Korteweg–de Vries (mKdV) equation. Phys Lett A. 2019; 383(14): 1578-82. https://doi.org/10.1016/j.physleta.2019.02.031

[33] Ahmed MS, Zaghrout A, Ahmed H. Construction of solitons and other solutions for NLSE with Kudryashov's generalized nonlinear refractive index. Alex Eng J. 2023; 64: 391-7. https://doi.org/10.1016/j.aej.2022.09.015

[34] Arnous AH, Mirzazadeh M, Akbulut A, Akinyemi L. Optical solutions and conservation laws of the Chen–Lee–Liu equation with Kudryashov's refractive index via two integrable techniques. Waves Random Complex Media. 2025; 35(2): 2607-23. https://doi.org/10.1080/17455030.2022.2045044

[35] Akinyemi L. Two improved techniques for the perturbed nonlinear Biswas–Milovic equation and its optical solitons. Optik. 2021; 243: 167477. https://doi.org/10.1016/j.ijleo.2021.167477

[36] Shehab MF, El-Sheikh MMA, Mabrouk AAG, Ahmed HM. Dynamical behavior of solitons with Kudryashov's quintuple power-law of refractive index having nonlinear chromatic dispersion using improved modified extended tanh-function method. Optik. 2022; 266: 169592. https://doi.org/10.1016/j.ijleo.2022.169592

[37] Zhang F, Hu Y, Liu H. Lie symmetry analysis, exact solutions, conservation laws of variable-coefficients Calogero–Bogoyavlenskii–Schiff equation. Int J Geom Methods Mod Phys. 2022; 19(2): 2250022. https://doi.org/10.1142/S0219887822500220

[38] Akram G, Sadaf M, Arshed S, Latif R. Exact traveling wave solutions of (2+1)-dimensional extended Calogero–Bogoyavlenskii–Schiff equation using extended trial equation method and modified auxiliary equation method. Opt Quantum Electron. 2024; 56(3): 424. https://doi.org/10.1007/s11082-023-05900-8

[39] Rayhanul Islam SM, Akbulut A, Yiasir Arafat SM. Exact solutions of the different dimensional CBS equations in mathematical physics. Partial Differ Equ Appl Math. 2022; 5: 100320. https://doi.org/10.1016/j.padiff.2022.100320

[40] Moatimid GM, El-Shiekh RM, Al-Nowehy AGA. Exact solutions for Calogero–Bogoyavlenskii–Schiff equation using symmetry method. Appl Math Comput. 2013; 220: 455-62. https://doi.org/10.1016/j.amc.2013.06.034

[41] Wazwaz AM. Multiple-soliton solutions for the Calogero–Bogoyavlenskii–Schiff, Jimbo–Miwa and YTSF equations. Appl Math Comput. 2008; 203(2): 592-7. https://doi.org/10.1016/j.amc.2008.05.004

[42] Kumar S, Malik S. A new analytic approach and its application to new generalized Korteweg–de Vries and modified Korteweg–de Vries equations. Math Methods Appl Sci. 2024; 47(14): 11709-26. https://doi.org/10.1002/mma.10150

[43] Ahmad J, Akram S, Ali A. Analysis of new soliton type solutions to generalized extended (2+1)-dimensional Kadomtsev–Petviashvili equation via two techniques. Ain Shams Eng J. 2024; 15(1): 102302. https://doi.org/10.1016/j.asej.2023.102302

[44] Karaman B. The use of improved-F expansion method for the time-fractional Benjamin–Ono equation. Rev R Acad Cienc Exactas Fís Nat Ser A Mat. 2021; 115(3): 128. https://doi.org/10.1007/s13398-021-01072-w

[45] Ding Y, He B, Li W. An improved F-expansion method and its application to the Zhiber–Shabat equation. Math Methods Appl Sci. 2012; 35(4): 466-73. https://doi.org/10.1002/mma.1574

[46] He Y. New Jacobi elliptic function solutions for the Kudryashov–Sinelshchikov equation using improved F-expansion method. Math Probl Eng. 2013; 2013(1): 104894. https://doi.org/10.1155/2013/104894

[47] Rui W. Applications of homogenous balanced principle on investigating exact solutions to a series of time fractional nonlinear PDEs. Commun Nonlinear Sci Numer Simul. 2017; 47: 253-66. https://doi.org/10.1016/j.cnsns.2016.11.018

[48] Wu C, Rui W. Method of separation variables combined with homogenous balanced principle for searching exact solutions of nonlinear time-fractional biological population model. Commun Nonlinear Sci Numer Simul. 2018; 63: 88-100. https://doi.org/10.1016/j.cnsns.2018.03.009

[49] Ren R, Zhang S, Rui W. Applications of homogenous balance principles combined with fractional calculus approach and separate variable method on investigating exact solutions to multidimensional fractional nonlinear PDEs. Math Probl Eng. 2020; 2020(1): 9101982. https://doi.org/10.1155/2020/9101982

[50] Zhang Y, Mei J, Hon YC. Exact soliton solutions of the discrete modified Korteweg–de Vries (mKdV) equation. Phys Essays. 2010; 23(2): 276-82. https://doi.org/10.4006/1.3371247

Appendix A: Summary of Representative Exact Solutions

The following table summarizes the representative exact solutions derived in this study, encompassing hyperbolic, trigonometric, and rational localized wave structures. To maintain compactness in the table, the variable $\xi = x + \omega y - rt$ represents the traveling wave parameter.

Table 1: Summary of representative exact solutions.

Eq. No.	Type	Exact Solution Expression $u(x, y, t)$
(48) ($u_{2.1.1}$)	Hyperbolic	$\lambda_1\xi + \frac{3}{(a+b)}\sqrt{\frac{-h_3}{\beta_1}}\tanh\left(\frac{\sqrt{-\beta_1 h_3}}{4\beta_1}\xi\right) + C$
(50) ($u_{2.1.2}$)	Hyperbolic	$\lambda_1\xi + \frac{3}{(a+b)}\sqrt{\frac{-h_3}{\beta_1}}\coth\left(\frac{\sqrt{-\beta_1 h_3}}{4\beta_1}\xi\right) + C$
(52) ($u_{2.2.1}$)	Trigonometric	$\lambda_1\xi - \frac{3}{(a+b)}\sqrt{\frac{h_3}{\beta_1}}\tan\left(\frac{\sqrt{\beta_1 h_3}}{4\beta_1}\xi\right) + C$
(54) ($u_{2.2.2}$)	Trigonometric	$\lambda_1\xi + \frac{3}{(a+b)}\sqrt{\frac{h_3}{\beta_1}}\cot\left(\frac{\sqrt{\beta_1 h_3}}{4\beta_1}\xi\right) + C$
(56) ($u_{3.1.1}$)	Hyperbolic	$\lambda_2\xi + \frac{3}{(a+b)}\sqrt{\frac{h_3}{2\beta_1}}\tanh\left(\frac{\sqrt{2\beta_1 h_3}}{4\beta_1}\xi\right) + C$
(58) ($u_{3.2.1}$)	Hyperbolic	$\lambda_2\xi + \frac{3}{(a+b)}\sqrt{\frac{h_3}{2\beta_1}}\coth\left(\frac{\sqrt{2\beta_1 h_3}}{4\beta_1}\xi\right) + C$
(60) ($u_{3.3.1}$)	Trigonometric	$\lambda_2\xi + \frac{6}{(a+b)}\sqrt{\frac{-h_3}{2\beta_1}}\tan\left(\frac{\sqrt{-2\beta_1 h_3}}{4\beta_1}\xi\right) + C$
(62) ($u_{3.3.2}$)	Trigonometric	$\lambda_2\xi - \frac{6}{(a+b)}\sqrt{\frac{-h_3}{2\beta_1}}\cot\left(\frac{\sqrt{-2\beta_1 h_3}}{4\beta_1}\xi\right) + C$
(73) ($u_{4.1.1.1}$)	Hyperbolic	$\frac{12p^2}{(a+b)(p-\sqrt{-\tau})}\left(\tau\xi + \sqrt{p}(-\tau)^{1/4}\tanh^{-1}\left(\frac{(-\tau)^{1/4}}{\sqrt{p}}\tanh(\sqrt{-\tau}\xi)\right)\right) + C$
(75) ($u_{4.1.1.2}$)	Hyperbolic	$\frac{12p^2}{a+b}\left(\sqrt{-\tau}\xi - \frac{\sqrt{p}}{\sqrt{p-\sqrt{-\tau}}}\tanh^{-1}\left(\frac{\sqrt{p}\tanh(\sqrt{-\tau}\xi)}{\sqrt{p-\sqrt{-\tau}}}\right)\right) + C$
(77) ($u_{4.1.2.1}$)	Trigonometric	$\frac{12p^2}{(a+b)(p-\sqrt{\tau})}\left(\tau\xi - \sqrt{p}\tau^{1/4}\arctan\left(\frac{\tau^{1/4}}{\sqrt{p}}\tan(\sqrt{\tau}\xi)\right)\right) + C$

(79) ($u_{4.1.2.2}$)	Trigonometric	$\frac{12p^2}{(a+b)(p+\sqrt{\tau})}\left(\tau\xi+\sqrt{p}\tau^{1/4}\tanh^{-1}\left(\frac{\sqrt{p}}{\tau^{1/4}}\tan(\sqrt{\tau}\xi)\right)\right)+C$
(81) ($u_{4.1.3.1}$)	Rational	$\frac{12p}{(a+b)(p\xi-1)}+C$
(84) ($u_{4.2.1.1}$)	Hyperbolic	$\frac{12\tau}{a+b}\left(\xi-\frac{1}{\sqrt{-\tau}}\tanh(\sqrt{-\tau}\xi)\right)+C$
(86) ($u_{4.2.1.2}$)	Hyperbolic	$\frac{12\tau}{a+b}\left(\frac{\xi}{2}+\frac{1}{4\sqrt{-\tau}}\sinh(2\sqrt{-\tau}\xi)\right)+C$
(88) ($u_{4.2.2.1}$)	Trigonometric	$-\frac{12\tau}{a+b}\left(\frac{1}{\sqrt{\tau}}\tan(\sqrt{\tau}\xi)-\xi\right)+C$
(90) ($u_{4.2.2.2}$)	Trigonometric	$\frac{12\tau}{a+b}\left(\xi+\frac{1}{\sqrt{\tau}}\cot(\sqrt{\tau}\xi)\right)+C$
(92) ($u_{4.2.3.1}$)	Rational	$\frac{12}{(a+b)\xi}+C$

Appendix B: Comparison with Representative Solutions from the Literature

To highlight our novelty, Table **2** compares our findings with representative solutions from [39, 40, 41]. These prior works employ fundamentally different techniques—the $exp(-\Phi(\zeta))$ expansion, Lie symmetry reduction, and Hirota's bilinear methods—yielding solution forms structurally and parametrically distinct from our kink, periodic, and rational wave families.

Table 2: Comparison of representative exact solutions.

Source	Method	Representative Solution Expressions
Ref. [39]	$exp(-\Phi(\zeta))$ expansion	$u=\dfrac{-4\mu}{\sqrt{\lambda^2-4\mu}\tanh\left(\dfrac{(\zeta_1+k)\sqrt{\lambda^2-4\mu}}{2}\right)+\lambda}+C$
$u=\dfrac{2\lambda}{e^{\lambda(\zeta_2+k)}-1}+C$		
Ref. [40]	Lie symmetry reduction	$u=\left(t+\frac{c_2}{3c_3}\right)^{-2/3}\left[A_0+\frac{1}{12}\left(x+z+\frac{c_6+c_5}{c_3}\right)^2\left(t+\frac{c_2}{3c_3}\right)^{-2/3}\right]-\frac{c_7}{c_3}$
$u=B_1e^{-c_3t}\sqrt{e^{2c_3t}\left(z-\frac{c_5}{2c_3}\right)}-\frac{c_7}{c_3}$		
Ref. [41]	Hirota bilinear	$u=\dfrac{2k_1e^{k_1x+m_1z-k_1^2m_1t}}{1+e^{k_1x+m_1z-k_1^2m_1t}}$
$u=2\left(\ln\left[1+e^{\theta_1}+e^{\theta_2}+\frac{(k_1-k_2)^2}{(k_1+k_2)^2}e^{\theta_1+\theta_2}\right]\right)_x$		
Present	Kumar–Malik / F-expansion	$u_{2.1.2}=\lambda_1\xi+\dfrac{3}{a+b}\sqrt{\dfrac{-h_3}{\beta_1}}\coth\left(\dfrac{\sqrt{-\beta_1h_3}}{4\beta_1}\xi\right)+C$
$u_{4.2.1.2}=\dfrac{12\tau}{a+b}\left(\dfrac{\xi}{2}+\dfrac{1}{4\sqrt{-\tau}}\sinh(2\sqrt{-\tau}\xi)\right)+C$		

Note: In Ref. [39], $\zeta_1=x+y-(\lambda^2-4\mu)t, \zeta_2=x+y-\lambda^2t$. In Ref. [41], $\theta_i=k_ix+m_iz-k_i^2m_it$ ($i=1,2$). In all tables, $\xi=x+\omega y-rt$.